HEAVY MESON SEMILEPTONIC DIFFERENTIAL DECAY RATE IN TWO DIMENSIONS IN THE LARGE Nc

Jorge Mondejar, Antonio Pineda and Joan Rojo

(hep-ph/0605248)

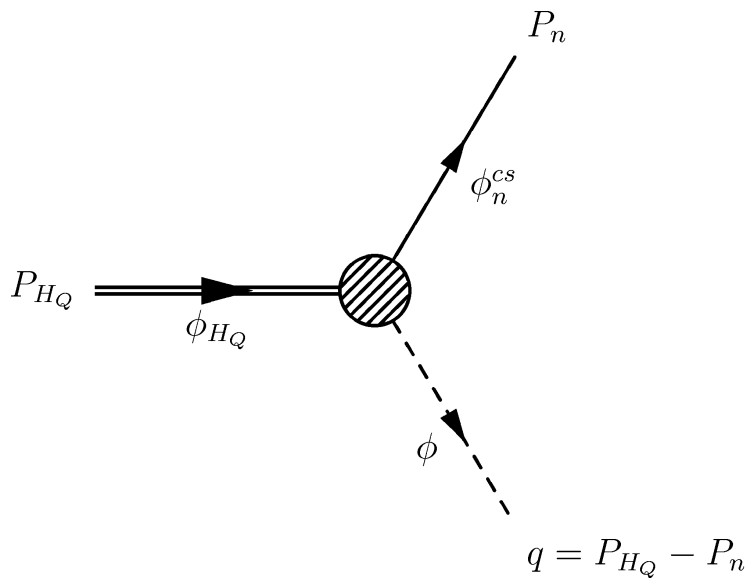

Figure 1: *Decay of the heavy meson H_Q to the meson $|cs;n\rangle$ and the fictitious ϕ particle.*

$$\mathcal{L}^V_{\text{weak}} = -\frac{G}{\sqrt{2\pi}}\bar{\psi}_c\gamma_\mu Q\epsilon^{\mu\nu}(\partial_\nu\phi) + (h.c.)\,,$$

$$\frac{d\Gamma^{(+)}}{dx} \equiv \frac{G^2 M_{H_Q}}{2(4\pi)^2} x Im T^{--}(q^- = 0, q^+)$$

with $x = q^+/M_{H_Q} \geq 0$, and

$$\frac{d\Gamma^{(-)}}{dx} \equiv \frac{G^2 M_{H_Q}}{2(4\pi)^2} x Im T^{++}(q^-, q^+ = 0)$$

with $x = q^-/M_{H_Q} \geq 0$.

$$T^{\mu\nu}(q) = \int d^2x e^{-iqx} i \left\langle H_Q | T \left\{ \bar{Q}(x)\gamma^\mu \psi_c(x)\, \bar{\psi}_c(0)\gamma^\nu Q(0) \right\} | H_Q \right\rangle ,$$

$$\frac{d\Gamma^{(+)}}{dx} = \frac{G^2 M_{H_Q}}{32\pi} \sum_{M_n \leq M_{H_Q}} \frac{x}{P^+_{H_Q}(1-x)} |\langle n; P^+_n | \bar{\psi}_c(0)\gamma^- Q(0) | H_Q \rangle|^2 \delta\left(P^-_{H_Q} - P^-_n\right) ,$$

$$\frac{d\Gamma^{(-)}}{dx} = \frac{G^2}{32\pi} \sum_{M_n \leq M_{H_Q}} x |\langle n; P^+_n | \bar{\psi}_c(0)\gamma^+ Q(0) | H_Q \rangle|^2 \delta\left(P^-_{H_Q} - P^-_n - q^-\right) .$$

Light-front quantization.

Impossible to get them from perturbation theory.

QCD_{1+1} in the light front

$$\mathcal{L}_{1+1} = -\frac{1}{4} G^a_{\mu\nu} G^{a,\mu\nu} + \sum_i \bar{\psi}_i \left(i\gamma^\mu D_\mu - m_i + i\epsilon \right) \psi_i \,,$$

where $D_\mu = \partial_\mu + igA_\mu$ and i labels the flavor.

x^+ =constant $\longrightarrow$ quantization frame ("time")

$P^- \longrightarrow$ Hamiltonian

P^+ kinetic variable.

$A^+ = 0$ gauge fixing

$$\mathcal{L} = \sum_i \psi^\dagger_{i+} i\partial^- \psi_{i+} + i \sum_i \frac{m_i^2 - i\epsilon}{4} \int dy^- \psi^\dagger_{i+}(x^-, x^+) \epsilon(x^- - y^-) \psi_{i+}(y^-, x^+)$$
$$+ \sum_{ij} \frac{g^2}{4} \int dy^- \psi^\dagger_{i+} t^a \psi_{i+}(x^-, x^+) |x^- - y^-| \psi^\dagger_{j+} t^a \psi_{j+}(y^-, x^+) \,,$$

$$P^- = -i \sum_i \frac{m_i^2 - i\epsilon}{4} \int dx^- dy^- \psi^\dagger_{i+}(x^-, x^+) \epsilon(x^- - y^-) \psi_{i+}(y^-, x^+)$$
$$- \sum_{ij} \frac{g^2}{4} \int dx^- dy^- \psi^\dagger_{i+} t^a \psi_{i+}(x^-, x^+) |x^- - y^-| \psi^\dagger_{j+} t^a \psi_{j+}(y^-, x^+) \,.$$

$$\boxed{P^- |n\rangle = P^-_n |n\rangle}$$

Large N_c

$$|ij;n\rangle = |ij;n\rangle^{(0)}$$
$$+ \sum_{m,n'} \sum_{k} |ik;n'\rangle^{(0)} |kj;m\rangle^{(0)(0)} \langle ik;n'|^{(0)} \langle kj;m|P^-|ij;n\rangle^{(0)} \frac{1}{P_n^{(0)-} - P_m^{(0)-} - P_{n'}^{(0)-}}$$
$$+ O\left(\frac{1}{N_c}\right) ,$$

Leading order in $1/N_c$

$$|ij;n\rangle^{(0)} = \frac{1}{\sqrt{N_c}} \int_0^{P_n^+} \frac{dp^+}{\sqrt{2(2\pi)}} \phi_n^{ij}\left(\frac{p^+}{P_n^+}\right) a_{i,\alpha}^\dagger(p) b_{j,\alpha}^\dagger(P_n - p)|0\rangle ,$$

By applying the operator P^- to its eigenstate $|n\rangle$ at leading order in $1/N_c$ one obtains the 't Hooft equation

$$M_n^2 \phi_n^{ij}(x) = \hat{P}^2 \phi_n^{ij}(x) \equiv \left(\frac{m_{i,R}^2}{x} + \frac{m_{j,R}^2}{1-x}\right) \phi_n^{ij}(x) - \beta^2 \int_0^1 dy \phi_n^{ij}(y) \mathrm{P} \frac{1}{(y-x)^2} ,$$

$$M_n^2 \simeq n\pi^2\beta^2 \qquad n \to \infty ,$$

$$m_{i,R} = m_i - \beta^2 \qquad \beta^2 = \frac{g^2 N_c}{2\pi}$$

Transition matrix elements

$$\langle cs;m|\bar{\psi}_c\gamma^+Q|Qs;n\rangle = 2\langle cs;m|\psi^\dagger_{+,c}Q_+|Qs;n\rangle = 2P_n^+(1-x)\left[\int_0^1 dz\phi_n^{Qs}(x+(1-x)z)\phi_m^{cs}(z)\right.$$
$$\left.-x^2\beta^2\int_0^1\int_0^1 dudz\frac{\phi_m^{cs}(z)G(u;q^2)}{(x(1-u)+(1-x)z)^2}(\phi_n^{Qs}(x+(1-x)z)-\phi_n^{Qs}(xu))\right],$$

$$G(u;q^2)\equiv\int_0^1 dv\sum_{n'=0}^{\infty}\frac{\phi_{n'}^{Qc}(u)\phi_{n'}^{Qc}(v)}{q^2-M_{n'}^2}.$$

$$\langle cs;m|\bar{\psi}_c\gamma^-Q|Qs;n\rangle = 2\langle cs;m|\left(\frac{m_c}{i\partial^+}\psi_{c,+}\right)^\dagger\left(\frac{m_Q}{i\partial^+}Q_+\right)|Qs;n\rangle$$
$$=\frac{2m_Qm_c}{P_n^+}\int_0^1 dz\frac{\phi_n^{Qs}(x+(1-x)z)\phi_m^{cs}(z)}{(x+(1-x)z)z}+2\beta^2\frac{1-x}{P_n^+}\sum_{n'=0}^{\infty}\frac{(-1)^{n'}M_{n'}^2}{q^2-M_{n'}^2}$$
$$\times\int_0^1\int_0^1\int_0^1 dydtdz\frac{\phi_{n'}^{Qc}(y)\phi_m^{cs}(t)\phi_{n'}^{Qc}(z)}{(t(1-x)+(1-z)x)^2}(\phi_n^{Qs}(x+(1-x)t)-\phi_n^{Qs}(xz)).$$

$$\langle cs;m|\bar{\psi}_cQ|Qs;n\rangle = \int_0^1 dz\phi_n^{Qs}(x+(1-x)z)\phi_m^{cs}(z)\left(\frac{m_Q(1-x)}{x+(1-x)z}+\frac{m_c}{z}\right)$$
$$-\beta^2\frac{x(1-x)}{m_Q-m_c}\sum_{n'\,\mathrm{odd}}\frac{M_{n'}^2}{q^2-M_{n'}^2}$$
$$\times\int_0^1\int_0^1\int_0^1 dydtdz\frac{\phi_{n'}^{Qc}(y)\phi_m^{cs}(t)\phi_{n'}^{Qc}(z)}{(t(1-x)+(1-z)x)^2}(\phi_n^{Qs}(x+(1-x)t)-\phi_n^{Qs}(xz)).$$

Disagreement with results by Burkardt and Swanson.

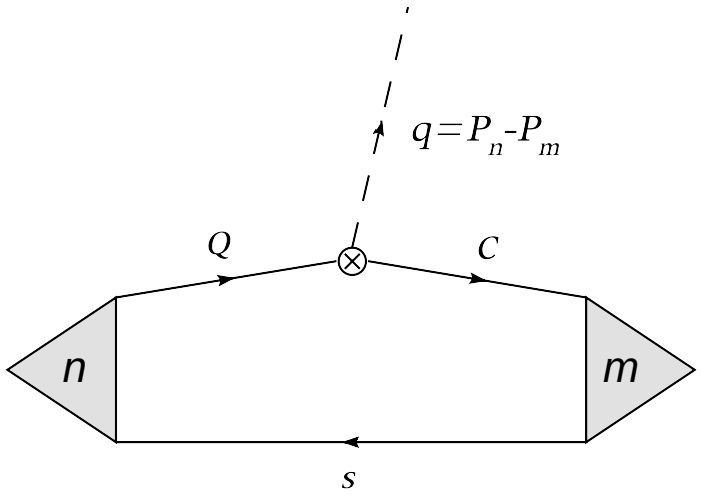

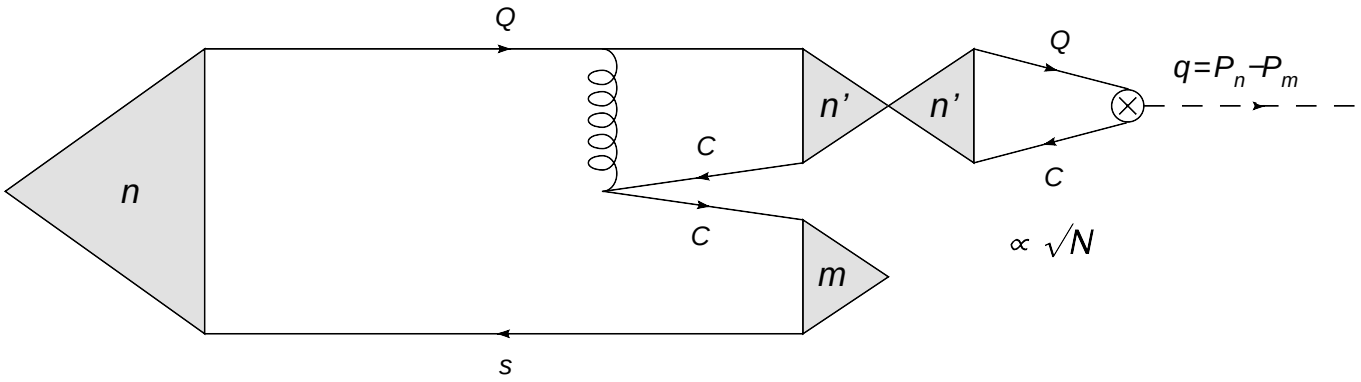

$\propto 1/\sqrt{N}$

$\propto \sqrt{N}$

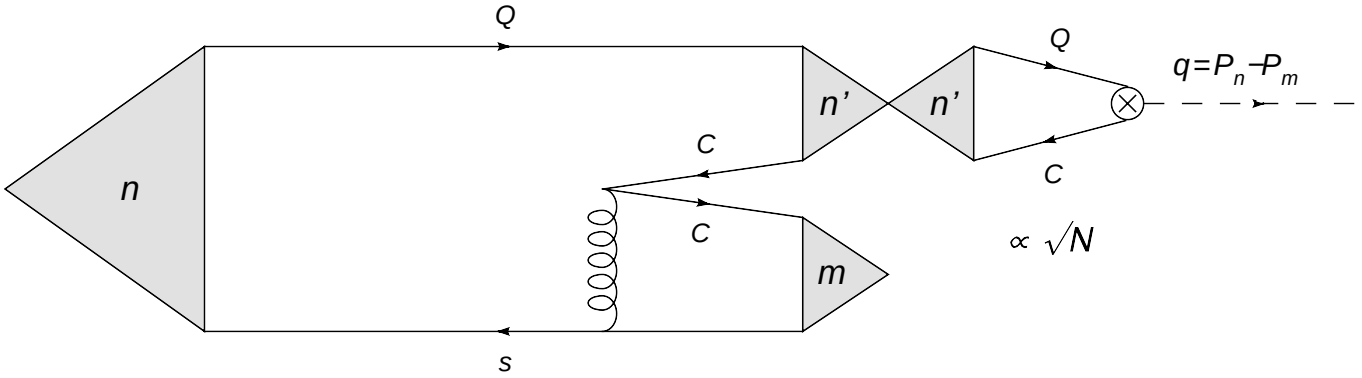

$\propto 1/\sqrt{N}$

$\propto \sqrt{N}$

Parity

$$\frac{d\Gamma^{(+)}}{dx} = \frac{d\Gamma^{(-)}}{dx} \equiv \frac{1}{2}\frac{d\Gamma}{dx}$$

$$\left| \int_0^1 dz \phi_n^{cs}(z)\phi_{H_Q}(z)\right| = \left|\frac{m_Q m_c}{(P_{H_Q}^+)^2}\int_0^1 dz \frac{\phi_{H_Q}(x_n+(1-x_n)z)\phi_n^{cs}(z)}{(x_n+(1-x_n)z)z}\right.$$

$$-\beta^2\frac{1-x_n}{(P_{H_Q}^+)^2}\sum_{n'=0}^{\infty}(-1)^{n'}\int_0^1\int_0^1\int_0^1 dydtdz\frac{\phi_{n'}^{Qc}(y)\phi_n^{cs}(t)\phi_{n'}^{Qc}(z)}{(t(1-x_n)+(1-z)x_n)^2}$$

$$\left.\times(\phi_{H_Q}(x_n+(1-x_n)t)-\phi_{H_Q}(x_n z))\right| .$$

Ok at the numerical level.

n	LHS	RHS ("diag" term)	Rel. Err.	RHS	Rel. Err.
0	0.96433	0.97144	$7\ 10^{-3}$	0.96627	$2\ 10^{-3}$
1	0.25999	0.26175	$6\ 10^{-3}$	0.26025	$1\ 10^{-3}$
2	0.04432	0.04473	$9\ 10^{-3}$	0.04445	$3\ 10^{-3}$
3	0.02389	0.02405	$7\ 10^{-3}$	0.02391	$1\ 10^{-3}$
4	0.00543	0.00538	$7\ 10^{-3}$	0.00540	$3\ 10^{-3}$

Table 1: *We take* $m_Q = 15\beta$, $m_c = 10\beta$ *and* $m_s = 0.56\beta$.

n	LHS	RHS ("diag" term)	Rel. Err.	RHS	Rel. Err.
0	0.46946	0.42992	$9\ 10^{-2}$	0.46493	$8\ 10^{-3}$
1	0.61406	0.62957	$2\ 10^{-2}$	0.61537	$2\ 10^{-3}$
2	0.49594	0.51617	$4\ 10^{-2}$	0.49821	$3\ 10^{-3}$
3	0.32820	0.34773	$6\ 10^{-2}$	0.32985	$5\ 10^{-3}$
4	0.18571	0.19712	$6\ 10^{-2}$	0.18694	$6\ 10^{-3}$

Table 2: *We take* $m_Q = 10\beta$, $m_c = \beta$, $m_s = \beta$.

Layer function

Previous work on the layer function: Einhorn (76); Brower, Spence and Weis (79)

a) OPE; $P_X^2 = M_n^2 = M_{H_Q}^2(1-x) \sim m_Q^2 \gg m_Q\Lambda_{QCD}$; $n \sim m_Q^2/g^2$,

b) SCETI; $P_X^2 = M_n^2 = M_{H_Q}^2(1-x) \sim m_Q\Lambda_{QCD}$; $n \sim m_Q/g$,

c) SCETII; $P_X^2 = M_n^2 = M_{H_Q}^2(1-x) \sim \Lambda_{QCD}^2$; $n \sim 1$.

$n \gg 1 \rightarrow$ OPE and SCETI

Semiclassical (WKB) solution to the bound state

$$\int_0^1 dz \phi_n^{cs}(z)\phi_{H_Q}(z) \simeq \pi\beta \frac{m_{Q,R}}{M_{H_Q}^2}\frac{1}{x}\phi_{H_Q}(x)\left(1+\frac{m_{c,R}^2}{m_{Q,R}^2}\left(\frac{\phi'_{H_Q}(x)}{\phi_{H_Q}(x)}-\frac{1}{x}\right)\right)\Big|_{x=x_n}.$$

$$\Gamma_n \overset{n\to\infty}{=} \frac{G^2 M_{H_Q}}{4\pi}\frac{m_{Q,R}^2}{M_{H_Q}^2}\frac{\pi^2\beta^2}{M_{H_Q}^2}\frac{1}{x_n}\phi_{H_Q}^2(x_n)\left[1+2\frac{m_{c,R}^2}{m_Q^2}\left(\frac{\phi'_{H_Q}(x_n)}{\phi_{H_Q}(x_n)}-\frac{1}{x_n}\right)+\cdots\right].$$

The differential decay rate then reads

$$\frac{d\Gamma^{(+)}}{dx} = \frac{1}{2}\sum_{M_n\le M_{H_Q}} \frac{G^2 M_{H_Q}}{4\pi}\frac{m_{Q,R}^2}{M_{H_Q}^2}\frac{\pi^2\beta^2}{M_{H_Q}^2}\frac{1}{x_n}\phi_{H_Q}^2(x_n)$$
$$\times\left[1+2\frac{m_{c,R}^2}{m_Q^2}\left(\frac{\phi'_{H_Q}(x_n)}{\phi_{H_Q}(x_n)}-\frac{1}{x_n}\right)+\cdots\right]\delta\left(x-1+\frac{M_n^2}{M_{H_Q}^2}\right).$$

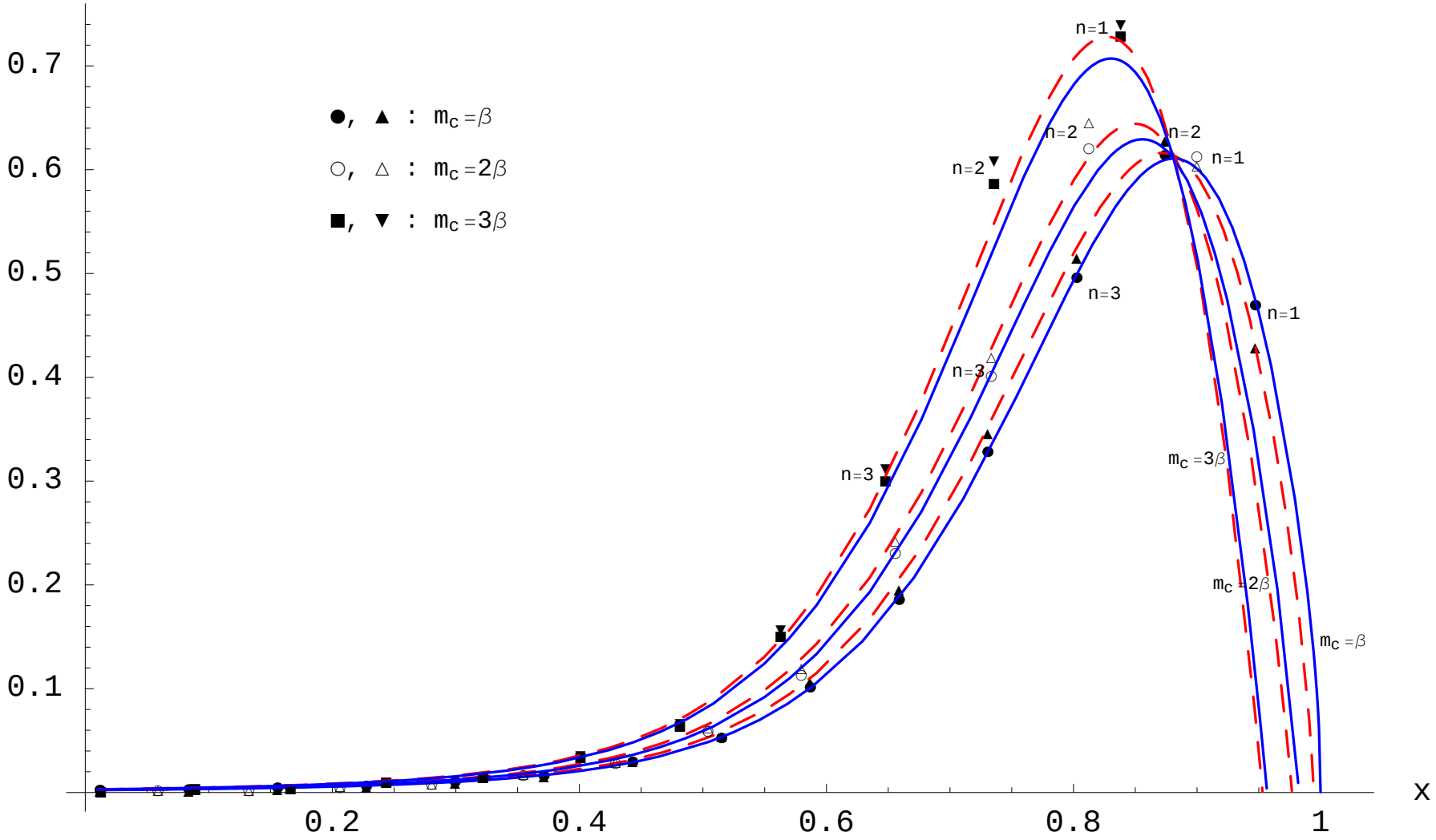
0.7
0.6
0.5
0.4
0.3
0.2
0.1
0.2
0.4
0.6
0.8
1
x
●, ▲ : mc =β
○, △ : mc =2β
■, ▼ : mc =3β
n=1
n=2
n=3
n=2
n=1
n=3
n=1
n=2
n=3
mc =3β
mc =2β
mc =β

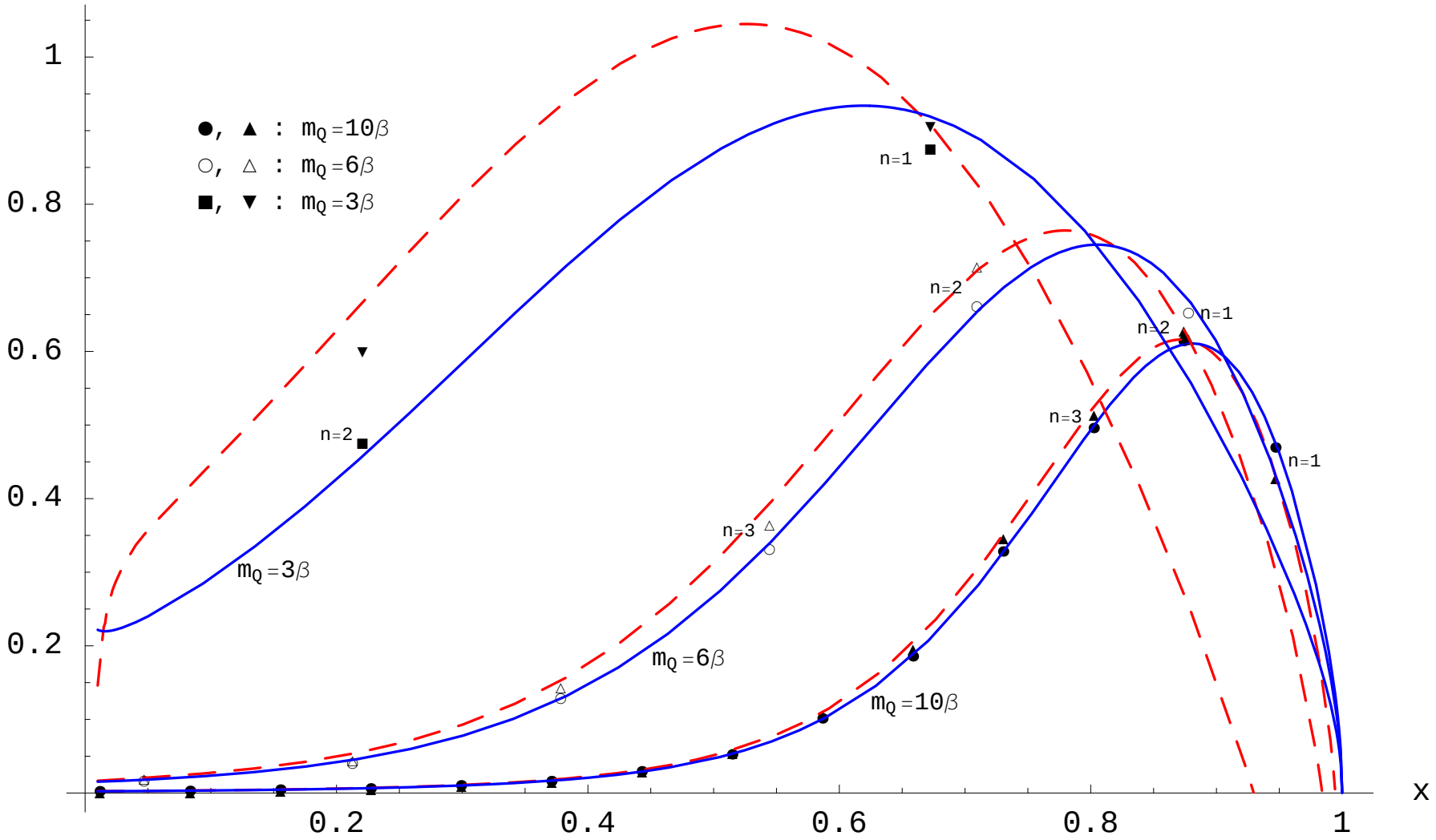
●, ▲ : $m_Q = 10\beta$
○, △ : $m_Q = 6\beta$
■, ▼ : $m_Q = 3\beta$
n=1
n=2
n=3
$m_Q = 3\beta$
$m_Q = 6\beta$
$m_Q = 10\beta$
1
0.8
0.6
0.4
0.2
0.2
0.4
0.6
0.8
1
x

Moments in the OPE ($N \sim 1$) and SCETI ($N\beta/m_Q \sim 1$) kinematic region

$$M_N \equiv \int_0^1 dx x^{N-1} \frac{d\Gamma}{dx} .$$

Use of the Euler-McLaurin formula: $\Sigma_n \longrightarrow \int dn$

$$M_N \simeq \frac{G^2 M_{H_Q}}{4\pi} \frac{m_{Q,R}^2}{M_{H_Q}^2} \left(1 - \frac{m_{c,R}^2}{m_{Q,R}^2}\right)^N \int_0^1 \frac{dx}{x^2} x^N \phi_{H_Q}^2(x) ,$$

$$\begin{aligned} M_N^{OPE} \simeq & \frac{G^2 m_Q}{4\pi} \left(1 - (N-1)\frac{\langle t \rangle}{m_Q} + \frac{(2N-1)\beta^2 - 2N m_c^2}{2m_Q^2} \right. \\ & \left. + \frac{(2(N-2)+3)\langle t \rangle^2 + ((N-2)(N-3)-3)\langle t^2 \rangle}{2m_Q^2} + O\left(\frac{1}{m_Q^3}\right)\right) . \end{aligned}$$

$$\begin{aligned} M_N^{SCETI} \simeq & \frac{G^2 M_{H_Q}}{4\pi} \frac{m_Q^2}{M_{H_Q}^2} \int_0^1 dx e^{-N(1-x)} \phi_Q^2(x) \\ & \times \left(1 + 2(1-x) - N\frac{(1-x)^2}{2} - N\frac{m_{c,R}^2}{m_Q^2} + + O\left(\frac{1}{m_Q^2}\right)\right) , \end{aligned}$$

Effective Field theories

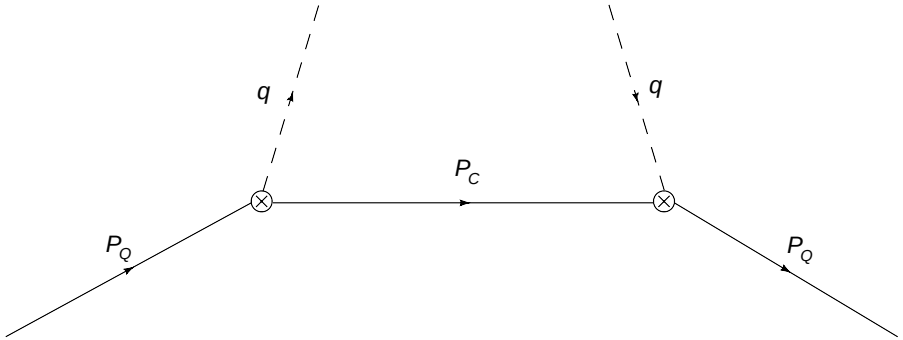

Figure 2: *Tree level diagram, the imaginary part of which gives the leading contribution to the effective vertex in the effective theory.*

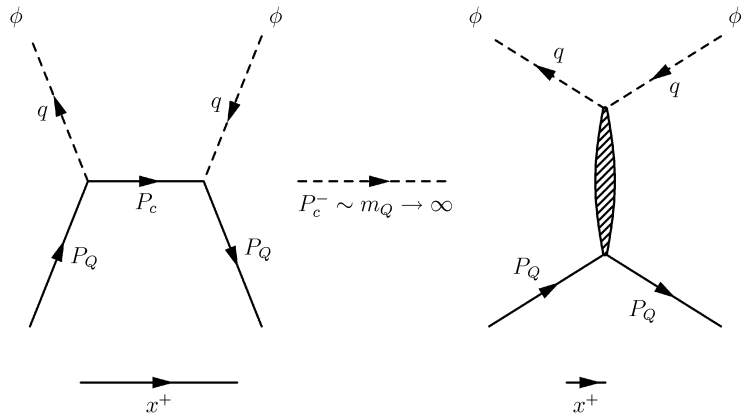

Figure 3: *Symbolic plot to represent the matching from QCD to the effective theory of the (tree-level) diagram, the imaginary part of which produces the decay of the heavy quark to a hard-collinear quark and the ϕ particle. The RHS of the figure represents the effective vertex in the effective theory. The shape of the effective vertex represents that it is local in x^+ but not in x^-.*

No need for hard-collinear particles. The interaction is (quasi-)local in x^+. The hard-collinear is not a dynamical degree of freedom.

SCETI $\longrightarrow$ HQET+imaginary vertex

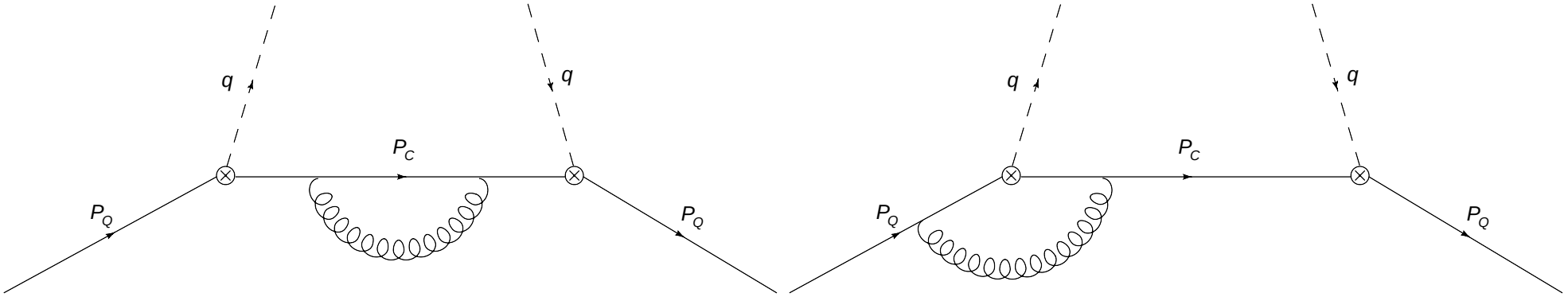

Figure 4: *One loop diagrams (plus their symmetrics), the imaginary part of which contribute to the effective vertex.*

$$\text{effective vertex} \sim \text{Im}\left[\frac{m_{c,R}^2}{P_c^2}\frac{m_{Q,R}^2}{(P_Q^+)^2}\frac{1}{P_c^+ - \frac{m_{c,R}^2-i\epsilon}{m_{Q,R}^2}P_Q^+}\right]$$
$$= -\pi\frac{m_{Q,R}^2}{(P_Q^+)^2}\delta\left(\left(1-\frac{m_{c,R}^2}{m_{Q,R}^2}\right)P_Q^+ - q^+\right),$$

$$\mathcal{L} = \mathcal{L}_{HQET} + Im[\mathcal{L}_I]$$

and the effective vertex reads

$$\mathcal{L}_I = -\frac{G^2}{2\pi}(\partial^+\phi)\left(\frac{m_{Q,R}}{i\partial^+}Q_+\right)^\dagger \frac{1}{i\partial^+ - \frac{m_{c,R}^2-i\epsilon}{m_{Q,R}^2}i\partial^+}\left(\frac{m_{Q,R}}{i\partial^+}Q_+\right)(\partial^+\phi^\dagger).$$

$$\frac{d\Gamma^{pert}}{dx} = \frac{1}{M_{H_Q}}\frac{1}{2(2\pi)x}\frac{G^2}{2\pi}(M_{H_Q}x)^2 2\mathrm{Im}T_{eff}$$

$$= \frac{G^2 M_{H_Q}}{4\pi}\frac{m_{Q,R}^2 - m_{c,R}^2}{m_{Q,R}^2}\left(\frac{m_{Q,R}^2}{M_{H_Q}^2}\right)\frac{1}{x}\phi_{H_Q}^2\left(\frac{x}{1-\frac{m_{c,R}^2}{m_{Q,R}^2}}\right) .$$

$$M_N^{pert} = \frac{G^2 M_{H_Q}}{4\pi}\frac{m_{Q,R}^2}{M_{H_Q}^2}\left(\frac{m_{Q,R}^2 - m_{c,R}^2}{m_{Q,R}^2}\right)^N \int_0^1 dx x^{N-2}\phi_{H_Q}^2(x) .$$

No violation of quark-hadron duality at the level of moments.

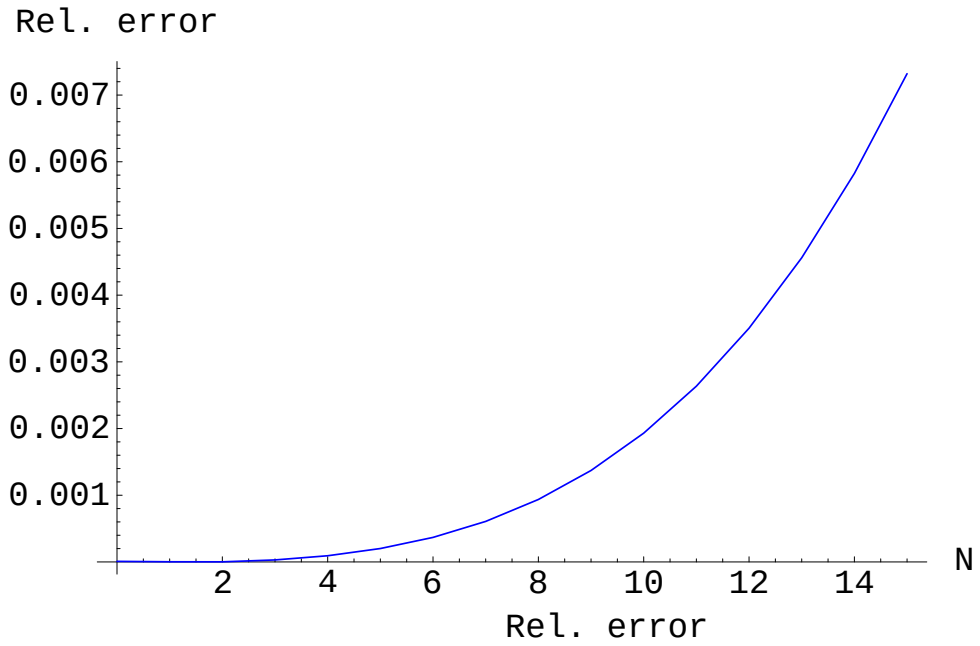

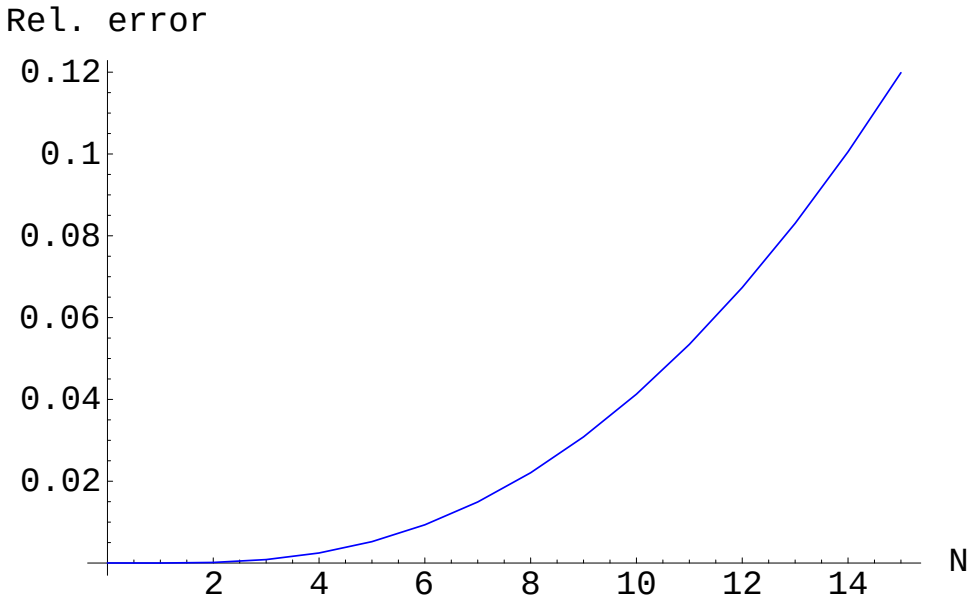

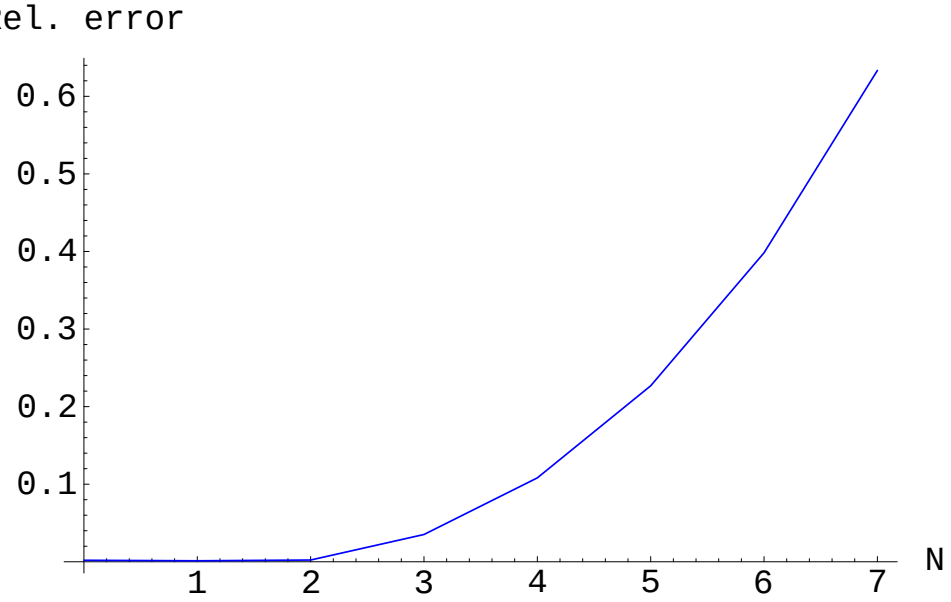

Figure 5: *Difference between the hadronic and perturbative result for the moments (divided by the hadronic result). The first figure is for the values* $m_Q = 10\beta$, $m_c = \beta$ *and* $m_s = \beta$, *the second is for the values* $m_Q = 15\beta$, $m_c = 10\beta$ *and* $m_s = 0.56\beta$ *and the third for the values* $m_Q = 3\beta$, $m_c = \beta$ *and* $m_s = \beta$.

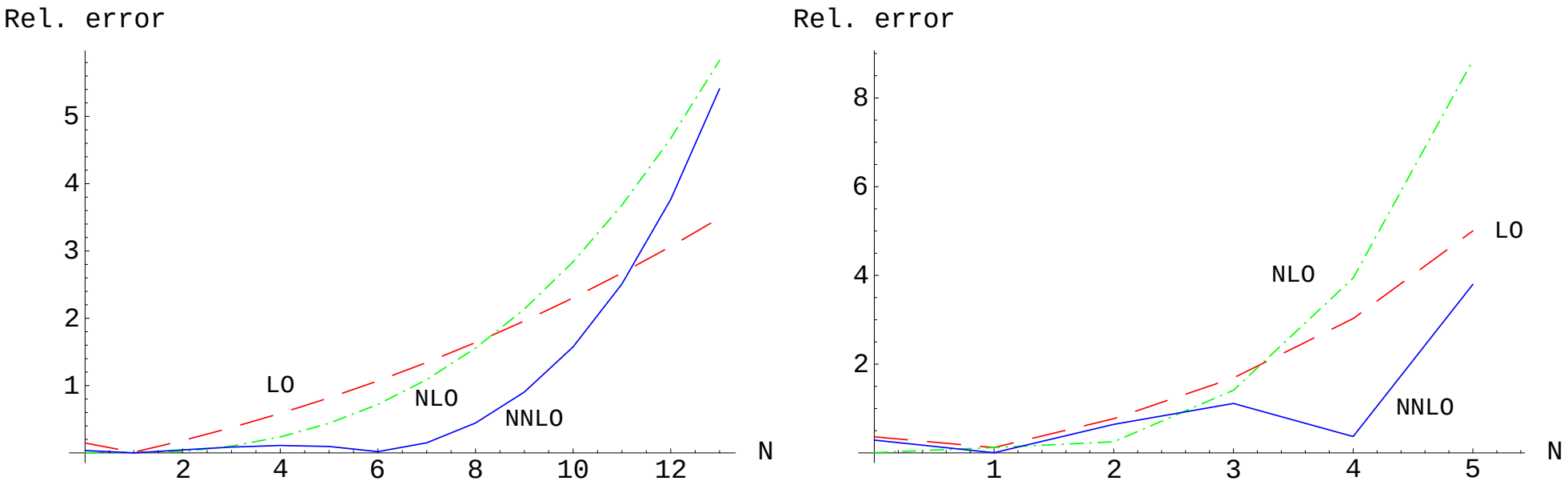

Figure 6: *Difference between the hadronic and perturbative result for the moments (divided by the hadronic result) in the OPE limit. The dashed line for the LO result, the dash-dotted line for the NLO result, and the solid line for the NNLO result. We take the values* $m_Q = 10\beta$, $m_c = \beta$ *and* $m_s = \beta$ *for the first figure and* $m_Q = 3\beta$, $m_c = \beta$ *and* $m_s = \beta$ *for the second figure. We use the values* $\langle t \rangle = 1.73\beta$ *and* $\langle t^2 \rangle = 3.99\beta^2$, *which can be checked with the sum rules of Burkardt and Uraltsev.*

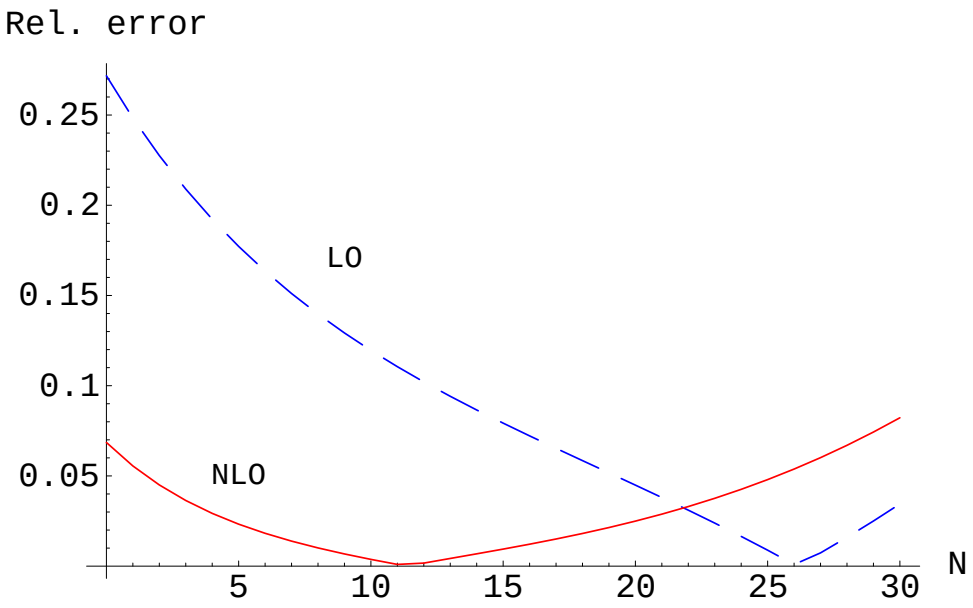

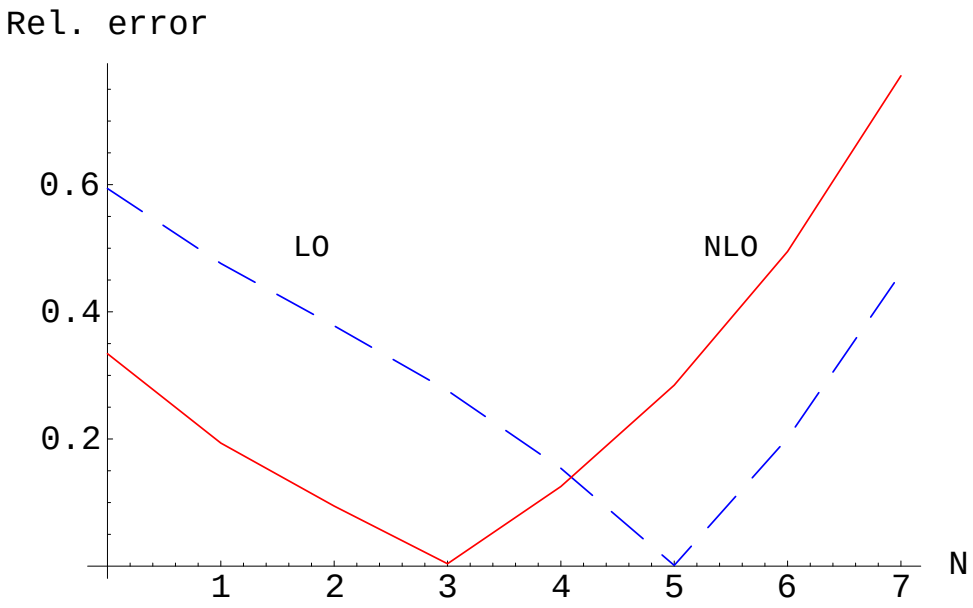

Figure 7: *Difference between the hadronic and perturbative result for the moments (divided by the hadronic result) in the SCETI limit. The dashed line for the LO result, and the solid line for the NLO result. We take the values* $m_Q = 10\beta$, $m_c = \beta$ *and* $m_s = \beta$ *for the first figure and* $m_Q = 3\beta$, $m_c = \beta$ *and* $m_s = \beta$ *for the second figure.*

Conclusions

Conclusions

Light-front Hamiltonian perturbation theory

Conclusions

Light-front Hamiltonian perturbation theory

We have computed the hadronic transition matrix elements

Conclusions

Light-front Hamiltonian perturbation theory

We have computed the hadronic transition matrix elements

$$\left.\frac{d\Gamma^{(+)}}{dx}\right|_{hadr.} \qquad \left.\frac{d\Gamma^{(-)}}{dx}\right|_{hadr.}$$

Conclusions

Light-front Hamiltonian perturbation theory

We have computed the hadronic transition matrix elements

$$\left.\frac{d\Gamma^{(+)}}{dx}\right|_{hadr.} \qquad \left.\frac{d\Gamma^{(-)}}{dx}\right|_{hadr.}$$

Approximated analytical results in the OPE and SCETI region ($n \gg 1$)

Conclusions

Light-front Hamiltonian perturbation theory

We have computed the hadronic transition matrix elements

$$\left.\frac{d\Gamma^{(+)}}{dx}\right|_{hadr.} \qquad \left.\frac{d\Gamma^{(-)}}{dx}\right|_{hadr.}$$

Approximated analytical results in the OPE and SCETI region ($n \gg 1$)

We have obtained the moments with relative accuracy of $O(\Lambda_{QCD}^2/m_Q^2)$ in the OPE kinematic region, and with relative accuracy of $O(\Lambda_{QCD}/m_Q)$ in the SCETI kinematic region.

Conclusions

Light-front Hamiltonian perturbation theory

We have computed the hadronic transition matrix elements

$$\left.\frac{d\Gamma^{(+)}}{dx}\right|_{hadr.} \qquad \left.\frac{d\Gamma^{(-)}}{dx}\right|_{hadr.}$$

Approximated analytical results in the OPE and SCETI region ($n \gg 1$)

We have obtained the moments with relative accuracy of $O(\Lambda_{QCD}^2/m_Q^2)$ in the OPE kinematic region, and with relative accuracy of $O(\Lambda_{QCD}/m_Q)$ in the SCETI kinematic region.

We have constructed and effective field theory local in x^+ without hard-collinear modes (therefore not equivalent to SCET)

Conclusions

Light-front Hamiltonian perturbation theory

We have computed the hadronic transition matrix elements

$$\left.\frac{d\Gamma^{(+)}}{dx}\right|_{hadr.} \qquad \left.\frac{d\Gamma^{(-)}}{dx}\right|_{hadr.}$$

Approximated analytical results in the OPE and SCETI region ($n \gg 1$)

We have obtained the moments with relative accuracy of $O(\Lambda^2_{QCD}/m^2_Q)$ in the OPE kinematic region, and with relative accuracy of $O(\Lambda_{QCD}/m_Q)$ in the SCETI kinematic region.

We have constructed and effective field theory local in x^+ without hard-collinear modes (therefore not equivalent to SCET)

$$\left.\frac{d\Gamma^{(+)}}{dx}\right|_{pert.} \qquad \left.\frac{d\Gamma^{(-)}}{dx}\right|_{pert.}$$

Conclusions

Light-front Hamiltonian perturbation theory

We have computed the hadronic transition matrix elements

$$\left.\frac{d\Gamma^{(+)}}{dx}\right|_{hadr.} \qquad \left.\frac{d\Gamma^{(-)}}{dx}\right|_{hadr.}$$

Approximated analytical results in the OPE and SCETI region ($n \gg 1$)

We have obtained the moments with relative accuracy of $O(\Lambda_{QCD}^2/m_Q^2)$ in the OPE kinematic region, and with relative accuracy of $O(\Lambda_{QCD}/m_Q)$ in the SCETI kinematic region.

We have constructed and effective field theory local in x^+ without hard-collinear modes (therefore not equivalent to SCET)

$$\left.\frac{d\Gamma^{(+)}}{dx}\right|_{pert.} \qquad \left.\frac{d\Gamma^{(-)}}{dx}\right|_{pert.}$$

Quark-hadron duality is not fulfilled at the $\frac{d\Gamma}{dx}$ level

Conclusions

Light-front Hamiltonian perturbation theory

We have computed the hadronic transition matrix elements

$$\left.\frac{d\Gamma^{(+)}}{dx}\right|_{hadr.} \qquad \left.\frac{d\Gamma^{(-)}}{dx}\right|_{hadr.}$$

Approximated analytical results in the OPE and SCETI region ($n \gg 1$)

We have obtained the moments with relative accuracy of $O(\Lambda^2_{QCD}/m^2_Q)$ in the OPE kinematic region, and with relative accuracy of $O(\Lambda_{QCD}/m_Q)$ in the SCETI kinematic region.

We have constructed and effective field theory local in x^+ without hard-collinear modes (therefore not equivalent to SCET)

$$\left.\frac{d\Gamma^{(+)}}{dx}\right|_{pert.} \qquad \left.\frac{d\Gamma^{(-)}}{dx}\right|_{pert.}$$

Quark-hadron duality is not fulfilled at the $\frac{d\Gamma}{dx}$ level

Quark-hadron duality is fulfilled at the level of moments with relative accuracy of $O(\Lambda^2_{QCD}/m^2_Q)$ in the OPE kinematic region, and with relative accuracy of $O(\Lambda_{QCD}/m_Q)$ in the SCETI kinematic region.